Changes in State of Stress on the Southern San Andreas Fault Resulting from the California Earthquake Sequence of April to June 1992

Steven C. Jaumé and Lynn R. Sykes

The April to June 1992 Landers earthquake sequence in southern California modified the state of stress along nearby segments of the San Andreas fault, causing a 50-kilometer segment of the fault to move significantly closer to failure where it passes through a compressional bend near San Gorgonio Pass. The decrease in compressive normal stress may also have reduced fluid pressures along that fault segment. As pressures are reequilibrated by diffusion, that fault segment should move closer to failure with time. That fault segment and another to the southeast probably have not ruptured in a great earthquake in about 300 years.

A series of large and moderate-size earthquakes struck southern California in April and June 1992 (hereafter referred to as the Landers earthquake sequence) to the north and northeast (Fig. 1) of San Gorgonio Pass (SGP). SGP is a tectonic knot where the San Andreas fault (SAF) changes direction (*1, 2*). In that region the SAF consists of several fault strands that accommodate strike-slip and reverse components of motion (*2–4*). The geometry of the bend makes plate motion more difficult there than along other sections of the plate boundary oriented more nearly parallel to the relative motion between the North American and Pacific plates. Higher tectonic stresses probably are required before sudden fault slip occurs in a larger earthquake in the vicinity of SGP. Earthquakes that break through that entire segment are likely to be characterized by long repeat times (a few hundred years), large displacements and seismic moments, and earthquake magnitudes **M** of 7.5 to 8.0; they would likely be great earthquakes, like the historic California shocks of 1857 and 1906. The SGP segment of the SAF probably has not broken in a great earthquake for at least 300 years. The adjacent Coachella Valley segment of the SAF between Palm Springs and the Salton Sea (Fig. 1) has also not ruptured in a great earthquake for about 300 years (*5, 6*).

In this report, we calculate the effect of the Landers series of earthquakes on the state of stress along segments of the SAF in southern California and discuss implications for the occurrence of future large to great earthquakes along one or more of those fault segments. Although only about half of the large (**M** > 7) historic earthquakes in southern California have occurred on the SAF, we concentrate our calculations on it because its long-term slip rate is high, its southernmost segments have not ruptured in about 300 years, and it is close to major metropolitan areas.

We modeled slip in the three earthquakes of April and June 1992 as dislocations in an elastic medium and calculated changes in stress (*7*) at closely spaced points at a depth of 7.5 km along the southernmost 190 km of the SAF (heavy line in Fig. 1). Shear and normal stress were calculated for a plane locally tangent to the fault at each of those points. The three earthquakes (Fig. 1) were represented as vertical dislocations extending from the surface to a depth of 10 km (*8*). We used a rigidity of 35 GPa and a Poisson's ratio of 0.25 in the calculations. The amount of slip in those events was chosen to match estimates of seismic moment, M_0, for each earthquake (*10*). The modeled dislocations are by necessity an oversimplification of the actual faulting in the Landers sequence. Nevertheless we feel that our calculations provide a good first approximation to the stress changes on the SAF resulting from this earthquake sequence.

Northwest and southeast of the SGP region the active trace of the SAF is well defined, and movements are believed to be largely strike slip on a nearly vertical fault (*2*). We modeled the fault in these areas as a vertical strike-slip fault. In the SGP region (50 to 110 km in Fig. 1), however, the geometry of the active SAF is poorly known, especially at depth. At the surface the SAF is multibranched and involves fault segments that show either strike-slip or reverse motion or combinations of the two (*2, 4*). Within the SGP region we performed calculations for a single continuous fault situated between the Mission Creek and Banning faults assuming three types of motion—strike slip on a vertical fault, strike slip on a fault dipping 45° to the northeast, and reverse slip on a 45° dipping fault. These three sets of calculations cover the ranges of behavior to be expected for major faults of the San Andreas system in that region.

To determine the extent to which various sections of the SAF moved toward failure, that is, the occurrence of frictional sliding in an earthquake, it is necessary to take into account changes in both shear stress, τ, and normal stress, σ. We determined the change in the Coulomb failure function, CFF

$$\Delta CFF = \Delta\tau - \mu\Delta\sigma_{\text{eff}} = \Delta\tau - \mu(\Delta\sigma - \Delta p)$$

where p is the fluid pressure, $(\sigma - p) = \sigma_{\text{eff}}$ is the effective or intergranular stress, μ is

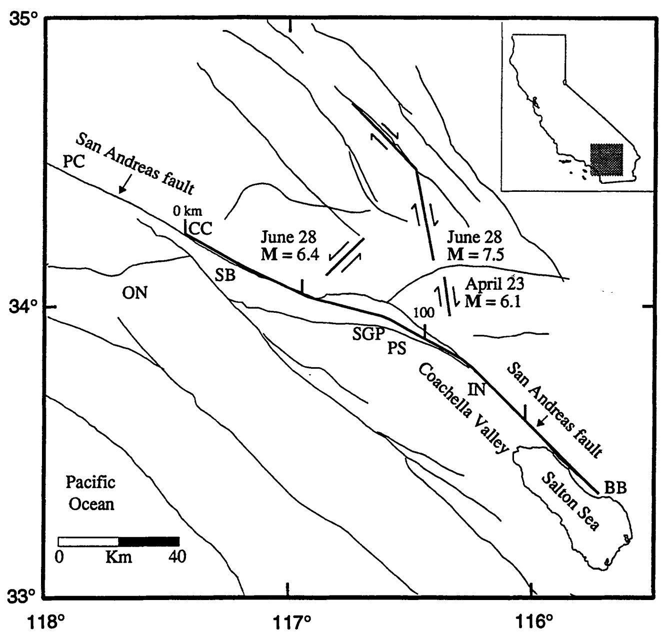

Fig. 1. Major faults (*23*) of southern California in vicinity of earthquakes in April and June 1992. Location within California shown by inset at upper right. Heavy lines with arrows indicate location, strike, and sense of slip in the three labeled earthquakes of 1992 (*10*) for which dislocations models were used to calculate stress changes. Portions of San Andreas fault for which stress changes were calculated are shown by the heavy line with tick marks every 50 km. Distances along San Andreas fault correspond to those of Fig. 2; SGP, San Gorgonio Pass. Paleoseismic sites: PC, Pallet Creek; CC, Cajon Creek; and IN, Indio. Place names: ON, Ontario; SB, San Bernadino; PS, Palm Springs; and BB, Bombay Beach.

Lamont-Doherty Geological Observatory and Department of Geological Sciences, Columbia University, Palisades, NY 10964.

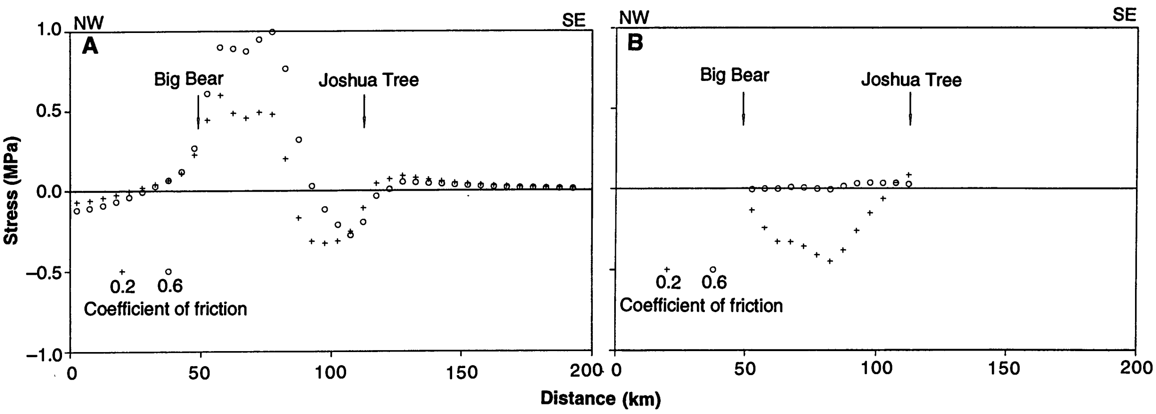

Fig. 2. Change in Coulomb failure function, ΔCFF, as a function of distance along San Andreas fault zone. Distances along fault correspond to those in Fig. 1. Positive values of ΔCFF promote (**A**) right-lateral strike-slip motion on a vertical fault or (**B**) reverse slip on faults dipping 45° northeast; negative values inhibit fault slip. Arrows mark where the along strike projections of Joshua Tree and Big Bear ruptures intersect the San Andreas fault. We expect that ΔCFF will evolve in time from curve $\mu = 0.2$ soon after the Landers earthquake sequence to that marked $\mu = 0.6$ as fluid pressures reequilibrate.

the coefficient of friction, and Δ denotes changes in the above quantities (*11*). For the three cases, τ is taken to be the component of shear stress in the direction of fault movement. Positive values of ΔCFF indicate movement toward failure (toward the failure envelope on a Mohr diagram); negative values indicate movement away from failure.

Laboratory values for μ generally range from 0.6 to 0.85 (*12–14*). The lack of a heat flow anomaly over the SAF and changes in the direction of the maximum compressive stress with distance from the fault, however, indicate that effective stresses along the entire SAF are considerably lower than expected for those values of μ (*12, 13*). Other major faults of the SAF system, such as the Calaveras fault in the San Francisco Bay region, also show evidence for a low μ (*15*). A recent study (*11*) found that a μ of 0.2 ± 0.1 yielded the best correlation between stress changes on faults in the San Francisco Bay region caused by the 1989 Loma Prieta earthquake and changes in the rate of occurrence of small earthquakes before and after that event. The value 0.2 was obtained for the assumption that changes in fluid pressure were negligible ($\Delta\sigma = \Delta\sigma_{eff}$). We calculated ΔCFF assuming both an average, 0.6, and a low, 0.2, value of μ.

Our calculations for the southernmost 190 km of the SAF showed that the largest ΔCFF values occur along a 75-km segment between where the projected strikes of the faults producing the Big Bear and Joshua Tree earthquakes intersect the SAF (Fig. 2). For strike-slip motion on a vertical fault (Fig. 2A), the stress changes in the model would encourage failure along the northwestern 50 km of this segment and inhibit it along the remaining 25 km. The calculated absolute value of ΔCFF where failure is encouraged is two to three times (up to ~1 MPa = 10 bars) as large as that where it is inhibited. To the northwest and southeast, the stress changes are smaller; failure is encouraged along the SAF to the southeast of SGP (120 to 190 km in Figs. 1 and 2) and inhibited on the segment to the northwest (0 to 30 km).

For strike-slip motion on a 45° north-dipping fault in the SGP area (not shown in Fig. 2), we find a nearly identical pattern to that in Fig. 2A but with values of ΔCFF about 0.8 times those in Fig. 2A. Values of ΔCFF for reverse faulting on a fault dipping 45° to either the south or north in the SGP region (Fig. 2B) are sensitive to the value of μ. For $\mu = 0.2$, the reduction in shear stress dominates, and a reverse fault is moved away from failure. For $\mu = 0.6$, the reductions in normal and shear stresses nearly counterbalance one another, and as a result, there was almost no change in CFF. Values of ΔCFF for a fault dipping 45° to the north with components of both right-lateral strike slip and reverse motion lie between those in Figs. 2, A and B. Active strike-slip faults that lie nearly along strike and to the north of the Landers rupture zone are predicted to have moved closer to failure. The northern 50 km of the San Jacinto fault is calculated to have moved closer to failure by about 0.1 and 0.25 MPa for $\mu = 0.2$ and 0.6.

We have not explicitly considered the role of pore fluids in our calculations of ΔCFF, which would require a knowledge of Δp. We follow Rice (*13*) in associating the apparent low value of μ on the SAF with high fluid pressures and low values of σ_{eff}, and in concluding that the permeability in the plane of the SAF is much greater than that perpendicular to it. Field studies of ancient, exhumed faults of the SAF system support the existence of high fluid pressures and anisotropic permeability (*16*). Following Scholz (*14*), if the undrained Poisson's ratio is 1/3 and Skempton's coefficient is 1, the ratio $\Delta p/\Delta\sigma$ is 2/3 and $\Delta\sigma_{eff}/\Delta\sigma$ is 1/3 immediately after a sudden change in σ. Thus, a change in normal stress, $\Delta\sigma$, across a fault caused by an earthquake on a nearby fault results in an immediate change in σ_{eff} only about 1/3 as large. A further change in $\Delta\sigma_{eff}$ of the same sign and about twice as large would be expected to occur with time as fluid pressures are restored by diffusion to or near their former levels (Fig. 3). In this case the findings of Reasenberg and Simpson (*11*) would be consistent with a $\mu \sim 0.6$, provided the time, T, for fluid pressure reequilibration was greater than the length of time they examined (1.7 years after the Loma Prieta earthquake). Thus a significant time after the occurrence of a nearby perturbing earthquake, $\Delta\sigma_{eff}$ would approach $\Delta\sigma$, and Δp would tend to zero.

If our assumption of anisotropic permeability is correct, fluid diffusion in response to pressure gradients induced by the Landers sequence would occur primarily within the fault zone. The length of the SAF that experienced a significant normal stress decrease is approximately 60 km long; thus, the length scale for diffusion of about 30 km (assuming flow from both the northwest and southeast). Fluids could also migrate upward along fault segments that suffered drops in normal stress from near-horizontal faults that appear to be present at depths of 10 to 12 km in the SGP region (*4*). There are several cases where fluid flow induced by either reservoir impounding or fluid injection in deep wells appears to have triggered moderate to large earthquakes. In those areas the hypocenters of moderate to large earthquakes were within about 10 to 30 km of either the reservoir or injection well; all of those events appear to have occurred on preexisting faults along which fluids under pressure were communicated to the hypocenters (*17, 18*). The time elapsed between the date of either the reservoir first reaching its maximum height or pulses of high-pressure fluid injection in a deep well near the causative fault and the largest earthquake ranged from 2 to 6 years (*17, 18*). If the time delays derived from the

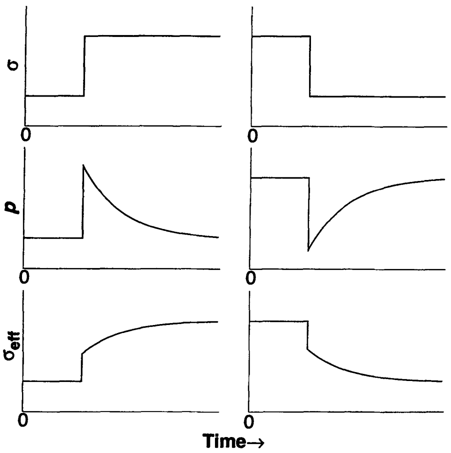

Fig. 3. Time-dependent changes in normal stress (σ), fluid pressure (p), and effective normal stress (σ_{eff}) across a fault zone before and after a major earthquake (sharp discontinuity in curves) along a nearby fault. An instantaneous change in σ is partitioned into a change in σ_{eff} and a change in p. With time fluid diffusion results in a return of p to its earlier value and, hence, in further change in σ_{eff}. Changes in p in a fault zone can result in it being either strengthened (**left**) or weakened (**right**) in terms of its frictional resistance to sliding. The instantaneous change in *CFF* is affected not only by the instantaneous change in σ_{eff} but also by the change in shear stress, τ. All further change in *CFF*, however, results from temporal changes in σ_{eff}.

above examples apply to the SGP segment, we would expect that reequilibration of fluid pressure would take at least 2 to 6 years. It is difficult to make an accurate estimate because so little is known about the permeability structure at depth beneath the SGP region.

If fluid pressure immediately dropped along faults in the SGP region as a result of the Landers sequence, then σ_{eff} would be expected to decrease in time like that shown on the right half of Fig. 3. If the actual value of μ is close to laboratory values and fluids are present at depth along the SAF of sufficient pressure to undergo changes of up to 0.5 MPa, the immediate response following the Landers sequence would be for the value of ΔCFF to lie near the curve $\mu = 0.2$ of Fig. 2. Thereafter, values of ΔCFF would evolve in time toward the line $\mu = 0.6$ as diffusion occurs. In this case more of the SAF in the SGP region would be moved toward failure with increasing time, and positive values of ΔCFF for strike-slip faulting in Fig. 2A would increase further. For a dipping fault with a reverse sense of slip (Fig. 2B), slippage would be stabilized by the immediate drop in shear stress and decrease in ΔCFF but then would move back with time toward the value of CFF that was present before the Landers sequence. More exact solutions must deal with poorly understood parameters like the presence of fluids and the permeability structure in fault zones.

Excavations of faults in the SGP area have not been successful in identifying a record of major prehistoric earthquakes breaking that region as yet. Evidence for three past ruptures of that area, however, may be obtained by correlating paleoseismic evidence from sites on either side of that region (*5*). Sediments deposited during the past 1000 to 2000 years and deformed in subsequent earthquakes have been examined in trenches excavated across the SAF at several sites (Fig. 1). Excavations near Indio indicate that the Coachella Valley segment, the southernmost 100 km of the SAF, has not ruptured since A.D. 1680 ± 40 and that the average repeat time of great earthquakes is about 200 to 300 years (*5*, *6*). Positive values of ΔCFF in Fig. 2A indicate that the central part of that segment near Indio moved closer to failure by a maximum of about 0.1 MPa (1 bar) as a result of the Landers sequence. Rupture in the great Fort Tejon earthquake of 1857 extended southeast only to a point between Pallet Creek and Cajon Creek (PC and CC in Fig. 1). Sedimentary disturbances related to a large (perhaps great) earthquake in 1812 are found at sites PC and CC but not at Indio (*5*). The 1812 event evidently ruptured to the southeast of site CC but did not break through the tectonic knot near SGP (*5*). It is not clear whether the shock at Indio about 1680 ruptured the entire length of the SAF shown in Fig. 1 and an additional 100-km segment to the northwest or only the Coachella Valley segment (*5*). It is possible that the SGP segment has not ruptured in a great shock since A.D. 1480 (*5*). In either case, however, it is likely a section of the SAF up to 140 km long has not ruptured in a great earthquake for about 300 years.

The northerly movement of the crustal block bounded by the SAF and the rupture zones of the Big Bear, southern Landers and Joshua Tree events permits plate motion to occur in the vicinity of the compressional bend of the SAF in and near SGP. The average shear stress that accumulates by plate motion and is suddenly released in a great plate boundary earthquakes is about 3 to 10 MPa (*19*); the maximum shear stress caused by the direct loading effect from large, deep reservoirs is about 1 MPa (*17*). The maximum values of the failure parameter ΔCFF in Fig. 2A, 0.5 and 0.9 MPa for values of μ of 0.2 and 0.6, are associated with near-vertical strike-slip faults over about a 30-km-long region within SGP. If fluid pressure reequilibrates in 2 to 6 years, we expect that stress on the SAF changed by 0.5 MPa at the time of the Landers sequence and will change by an additional 0.4 MPa in the next 2 to 6 years. For the complex SGP region we expect somewhat higher than normal average stress drops in great earthquakes. Hence, we adopt a value of 6 MPa. The maximum values of ΔCFF of 0.5 and 0.9 MPa represent about 8 and 15% of that stress drop. Assuming an average repeat time of 300 years for the SGP region (*5*, *6*), they represent the equivalent of about 25 and 45 years of typical slow stress accumulation. Those estimates may be uncertain by a factor of 2. Because we do not know the absolute values of stress, neither the current level nor the level at which a large shock is triggered, it is not clear if the calculated changes over the next decade will be sufficient to trigger a great earthquake. We can say that the chance of a great event happening somewhere along the southern 160 km of the SAF is greater after the Landers sequence than it was before.

Two scenarios for the next great earthquake along the southern SAF are likely: (i) the SGP and Coachella Valley segments break together in a single great event as they are inferred to have done (*5*) three times from the paleoseismic record; and (ii) the Coachella Valley segment ruptures alone as it is inferred to have done at least once (*5*) followed some time later, perhaps decades, by rupture of the SGP segment. Rupture in large earthquakes often stops at geometrical irregularities such as bends and offsets of the fault surface (*20*). Uncertainties about the date the SGP segment last ruptured in a great event and its average repeat time make it difficult to choose one of the two scenarios over the other. Thus, the major bend in the SAF near Palm Springs may arrest rupture in an event that is initiated in the Coachella Valley. Rupture of the SGP region may be arrested to the northwest where the fault that ruptured in the Big Bear shock intersects the SAF. Enough shear stress may not have reaccumulated along the segment of the SAF between San Bernadino and SGP since 1812 for an earthquake in SGP to propagate into that region. At the long-term slip rate of about 24 mm/year for that segment (*6*), stresses equivalent to 4.3 m of potential slip have accumulated since 1812. The size of that slip deficit indicates to us that it is more likely that a great event initiated in the SGP region is likely to rupture to the northwest as far as CC in Fig. 1 and perhaps farther.

The frequency of occurrence of **M** > 5 and **M** > 6 earthquakes has increase markedly in southern California since about 1986. That activity occurred mainly within the area of Fig. 1 and immediately to its south and west. Its spatial extent and increase with time resemble patterns of activity in the 25 years before large earthquakes in the San Francisco Bay area (*21, 22*). Unlike those examples the activity in southern California neither surrounded nor partly enclosed the rupture zone of the Landers earthquake itself. Instead, it mainly surrounds the southern SAF. Thus, the pattern probably was not precursory to the Landers event; that pattern plus the Landers sequence, may be part of a long-term precursor to a future great earthquake along the SAF. The high rate of moderate to large events is likely to continue. Activity for moderate-sized shocks decreased markedly in the Bay area after the 1906 earthquake and remained low for several decades, as seems to have been the case for decades after the great 1857 event in southern California (*21, 22*). These patterns can be attributed to a long period of regional stress increase without large to great shocks followed by a regional decrease in stress at or near the times of such events.

In the 8.5-year period before the Desert Hot Springs earthquake of 1948 (near kilometer 100 in Fig. 1) shocks of $4 < \mathbf{M} < 5.5$ occurred about 15 times more frequently within a radius of about 50 km of the hypocenter of that event than in similar other time intervals (*1, 22*). That burst of activity ended with the 1948 earthquake. The sizes of the shocks involved in that precursory sequence, and the area over which they occurred are much smaller than those for the pattern that has existed since about 1986. Sykes and Seeber (*1*) proposed that, given its structural complexity, it was unlikely that the major tectonic knot near SGP would rupture in a great earthquake without first undergoing major permanent deformation involving either rotations or translations of nearby crustal blocks. One of the two precursory scenarios that they suggested was that the sequence that preceded the 1948 shock may be a scaled-down version of the sequence that will lead to a great earthquake that ruptures either the SGP or Coachella Valley segments of the SAF. The occurrence of the Landers sequence, other activity since 1986, and the movement of the large crustal block to the north of SGP in that sequence bear strong resemblance to that scenario. It should be remembered, however, that the historic record is short enough that we do not have information on seismicity patterns preceding great earthquakes in this region.

It had been estimated (6) that the chance was about 60% that one or more great earthquakes would occur along the SAF in southern California from 1988 to 2018. We conclude that the increase in moderate to large earthquakes since 1986 and the changes in stress along the SAF associated with the Landers sequence indicate that the probability of a great shock is now higher than that estimated in 1988.

REFERENCES AND NOTES

1. L. R. Sykes and L. Seeber, *Geology* **13**, 835 (1985).
2. J. C. Matti, D. M. Morton, B. F. Cox, *U.S. Geol. Surv. Open-File Rep. 85-365* (1985).
3. C. R. Allen, *Geol. Soc. Am. Bull.* **68**, 315 (1957).
4. C. Nicholson, L. Seeber, P. Williams, L. R. Sykes, *J. Geophys. Res.* **91**, 4891 (1986).
5. K. Sieh, M. Stuiver, D. Brillinger, *ibid.* **94**, 603 (1989).
6. Working Group on California Earthquake Probabilities, *U.S. Geol. Surv. Open File Rep. 88-398* (1988).
7. L. Erickson, thesis, Stanford University (1986).
8. Earthquake hypocenters from the California Institute of Technology earthquake catalog in the San Bernadino Mountains–eastern Mojave Desert region show few earthquakes with depths greater than 12 km.
9. **M** is calculated using the formula $\mathbf{M} = 2/3 \log M_0 - 6.05$ (M_0 in Newton meters) modified from T. C. Hanks and H. Kanamori, *J. Geophys. Res.* **84**, 2348 (1979). Seismic moments, M_0, are from preliminary moment tensor solutions calculated by the Harvard group and reported in the "Preliminary Determination of Epicenters Catalog" (U.S. Geological Survey, Reston, VA); J. Mori, K. Hudnut, L. Jones, E. Hauksson, and K. Hutton [*Eos* **73**, 417 (1992)] reported that more recent estimates of the M_0 for the Landers earthquake are smaller than the original estimate.
10. The amount of slip in each event was chosen to match its preliminary seismic moment, given the assumed rupture area and rigidity. These average displacements were used for the following earthquakes in the 1992 sequence: 0.4 m, 23 April, Joshua Tree; 7.7 m, 28 June, Landers; 0.7 m, 28 June, Big Bear. The computed stresses are not greatly changed if the rupture depths are increased and the overall displacement decreased.
11. P. A. Reasenberg and R. W. Simpson, *Science* **255**, 1687 (1992).
12. A. H. Lachenbruch and A. McGarr, *U.S. Geol. Surv. Prof. Pap.* **1515**, 261 (1990).
13. J. R. Rice, in *Fault Mechanics and Transport Properties of Rock: a Festchrift in Honor of W. F. Brace*, B. Evans and T.-F. Wong, Eds. (Academic Press, San Diego, CA, 1992), pp. 475–503.
14. C. H. Scholz, *The Mechanics of Earthquakes and Faulting* (Cambridge Univ. Press, Cambridge, 1990), p. 328.
15. D. H. Oppenheimer, R. A. Reasenberg, R. W. Simpson, *J. Geophys. Res.* **93**, 9007 (1988).
16. F. M. Chester, J. P. Evans, R. L. Beigel, *ibid.*, in press.
17. D. W. Simpson, W. S. Leith, C. H. Scholz, *Bull. Seismol. Soc. Am.* **78**, 2025 (1988).
18. J. H. Healy, W. W. Rubey, D. T. Griggs, C. B. Raleigh, *Science* **161**, 1301 (1968).
19. C. H. Scholz, C. Aviles, S. Wesnousky, *Bull. Seismol. Soc. Am.* **76**, 65 (1986).
20. G. King and J. Nábělek, *Science* **228**, 984 (1985).
21. W. L. Ellsworth, *U.S. Geol. Surv. Prof. Pap.* **1515**, 153 (1990).
22. L. R. Sykes and S. C. Jaumé, *Nature* **348**, 595 (1990).
23. C. W. Jennings, fault map of California, Sacramento, California Division of Mines and Geology, scale 1:750,000 (1975).

24. We thank C. Scholz, L. Seeber, A. Nur, and an anonymous reviewer for critical reviews. Scholz pointed out to us literature on changes in fluid pressures in fault zones accompanying a change in normal stress. We thank J. Beavan for providing a copy of the computer program used for calculating changes in stress for planar dislocations. This work supported by grants from the U.S. Geological Survey and the Southern California Earthquake Center. Lamont-Doherty Geological Observatory contribution 5016.

10 August 1992; accepted 23 October 1992

Change in Failure Stress on the Southern San Andreas Fault System Caused by the 1992 Magnitude = 7.4 Landers Earthquake

Ross S. Stein, Geoffrey C. P. King,* Jian Lin*

The 28 June Landers earthquake brought the San Andreas fault significantly closer to failure near San Bernardino, a site that has not sustained a large shock since 1812. Stress also increased on the San Jacinto fault near San Bernardino and on the San Andreas fault southeast of Palm Springs. Unless creep or moderate earthquakes relieve these stress changes, the next great earthquake on the southern San Andreas fault is likely to be advanced by one to two decades. In contrast, stress on the San Andreas north of Los Angeles dropped, potentially delaying the next great earthquake there by 2 to 10 years.

The largest earthquake to strike southern California during the past four decades did not rupture the San Andreas fault, but instead slipped faults within the eastern California shear zone identified previously by geologic (*1*), geodetic (*2*), and mechanical (*3*) methods. Here we show that several smaller shocks that occurred near the Landers event during the preceding 17 years increased stress at the future Landers epicentral site and along much of the eventual rupture path. Similarly, we argue that the Landers earthquake and its aftershocks have changed the stress along the San Andreas fault system.

We used an elastic halfspace boundary

R. S. Stein, U.S. Geological Survey, Mail Stop 977, Menlo Park, CA 94025.
G. C. P. King, Institut de Physique du Globe, Strasbourg 67084, France.
J. Lin, Woods Hole Oceanographic Institution, Woods Hole, MA 02543.

*Visiting Fellows of the Southern California Earthquake Center.